Electronic Supplementary Material (ESI) for RSC Advances.

Supporting Information

In-situ grown amorphous ZrO_2 layer on zeolite for enhanced phosphates adsorption

Ying Tao, *[ab] Shaojia Liu,[c] Shizhi Dong,[a] Chengguo Wang,[b] Tao Qu,[b] Sinan Li, [b] Lingling Li[b] and Zhuang Ma *[ab]

a. College of Mining, Liaoning Technical University, Fuxin, 123000, P. R. China.
b. School of Metallurgy Engineering, Liaoning Key Laboratory of Optimization and Utilization of Non-associated Low-grade Iron Ore, Liaoning Institute of Science and Technology, Benxi, 117004, P. R. China.
c. School of Chemistry, Beihang University, Beijing 100191, P. R. China.

2. Materials and methods

2.4. Batch adsorption experiments

The quantification of phosphates concentrations were determined by Mo-Sb Anti-spectrophotometer method, which works as follows: orthophosphate reacts with ammonium molybdate and potassium antimonyl tartrate under acidic condition to give molybdophosphate heteropoly acid, which is further reduced by ascorbic acid to form the phosphomolybdenum blue complex. The limit of detection (i.e. LOD) of phosphorus concentration by this method is 0.01 mg/L.

Sulfuric acid solution was prepared by mixing analytical pure sulfuric acid (H_2SO_4, 95.0～98.0%) with deionized water at volume ratio of 1:1. 10% L-Ascorbic acid solution was prepared by dissolving 10 g L-Ascorbic acid ($C_6H_8O_6$, ≥99.7%) into some deionized water and then diluting to 100 mL in brown volumetric flask. Ammonium molybdate solution and potassium antimony oxide tartrate solution were prepared respectively by dissolving 13g ammonium molybdate ($(NH_4)_6Mo_7O_{24}\cdot 4H_2O$, ≥99.0%) and 0.35 g potassium antimony(Ⅲ) L-tartrate hemihydrate ($C_4H_4KO_7Sb\cdot 0.5H_2O$, ≥99.0%) into 100 mL deionized water. Both solutions were slowly added into 300 mL sulfuric acid solution with continuous stirring to obtain molybdate solution.

2-4 mL standard solution of phosphates with concentrations ranging from 0.2 to 1.2 mg/L was taken out from the flask and then filtered off using 0.45 μm membrane filters and diluted with deionized water in definite proportions. 1 mL L-Ascorbic acid solution was added into 50 mL sample solution and mixed well, and 2 mL molybdate solution was then added above solution after 30 s and sited for 15 min to color the solution. The absorbance of color solution was further determined on a Shimadzu UV-3600 UV-Vis spectrometer. Deionized water was used as reference liquid to achieve baseline correction of spectral signals before the test. Test parameters: wavelength: 700 nm; cuvette width: 10 mm; radiation source: iodine-tungsten lamp. The standard curve of phosphates concentration was obtained as Fig. S1. Based on the high related coefficient R^2 of 0.9999, the standard curve of phosphates with concentration ranging from 0.2~1.2 mg/L reveal excellent linear correlation with absorbance. Six test solutions were used to conduct three parallel tests and calculated the limit of detection (LOD) and limit of quantification (LOQ) by the mean average of absorbance, which were determined as 0.038 mg/L (LOD=3.3σ/S) and 0.116 mg/L (LOQ=10σ/S), respectively, where σ is the deviation of response value, S is the slope of standard curve. The relative standard deviation (RSD) was 0.8% in the measurement, showing a good precision. Likewise, the absorbance of test solution was detected by the same method and the residual phosphates concentration (C_t) after adsorption experiment was calculated by the standard curve.

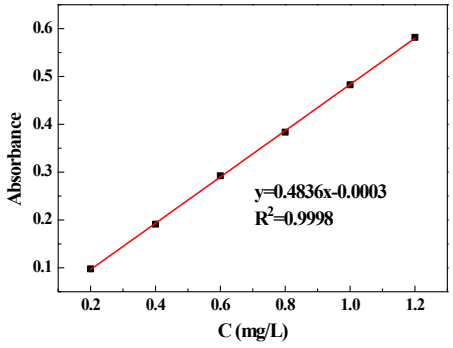

Fig. S1 Standard curve of phosphates concentration.

3. Results and discussion

3.1. Characterization of adsorbents

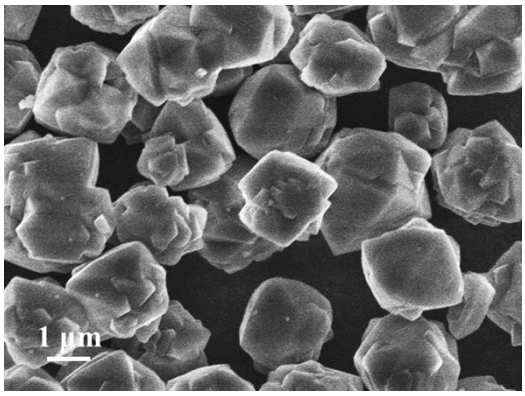

Fig. S2 SEM morphology of the pristine zeolite dissolved in deionized water.

As depicted in Fig. S2, the pristine zeolite possess the relatively regular near-spherical particles morphology, and can be uniformly dissolved in deionized water without any reunion.

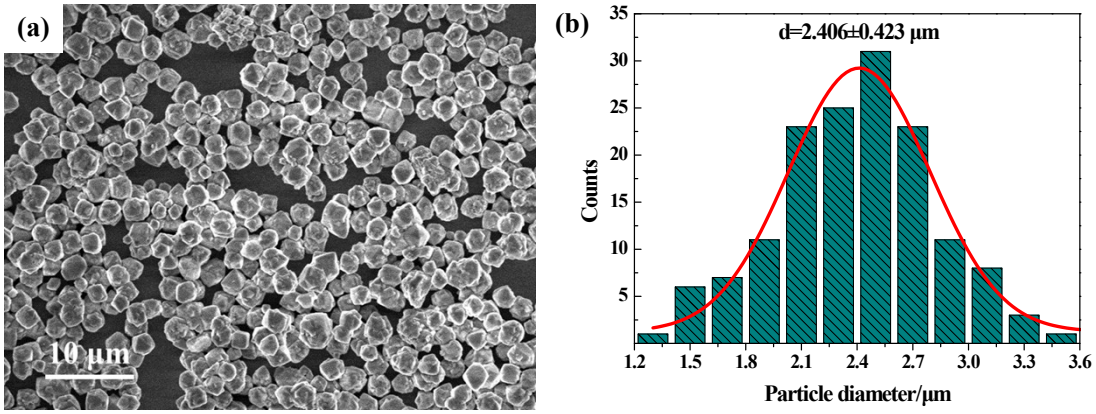

Fig. S3 SEM morphology of as-prepared ZEO@AZ adsorbent (a), and the particle diameter distribution and fitted curve (b) obtained by Image J software for statistical treatment on 150 randomly distributed particles in Fig. S3a.

Fig. S3a further reveals the low multiples SEM morphology of as-prepared ZEO@AZ adsorbent similar to that of the pristine zeolite (Fig. S2). Bar graph in Fig. S3b confirms that the diameters of ZEO@AZ particles in Fig. S3a are in line with normal curve of distribution with the average diameter of 2.406±0.423 μm.

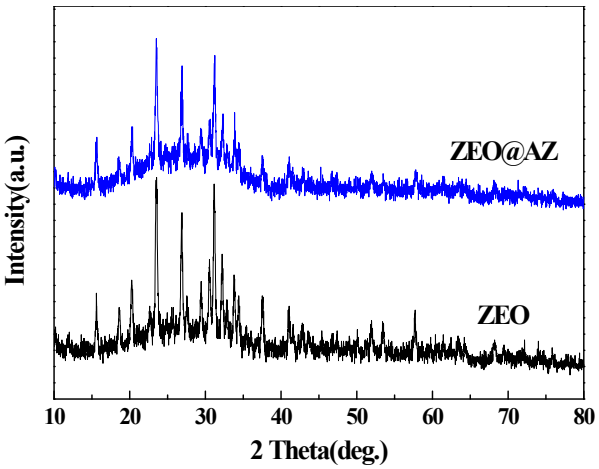

Fig. S4 XRD pattern of ZEO@AZ and ZEO samples.

As shown in Fig. S4, the XRD diffraction pattern of ZEO sample is well-indexed with zeolite (JCPDS No. 38-0232). Meanwhile, the characteristic peaks of ZEO@AZ are basically consistent with those of the initial zeolite. Therefore, ZrO_2 in ZEO@AZ is considered to be amorphous.

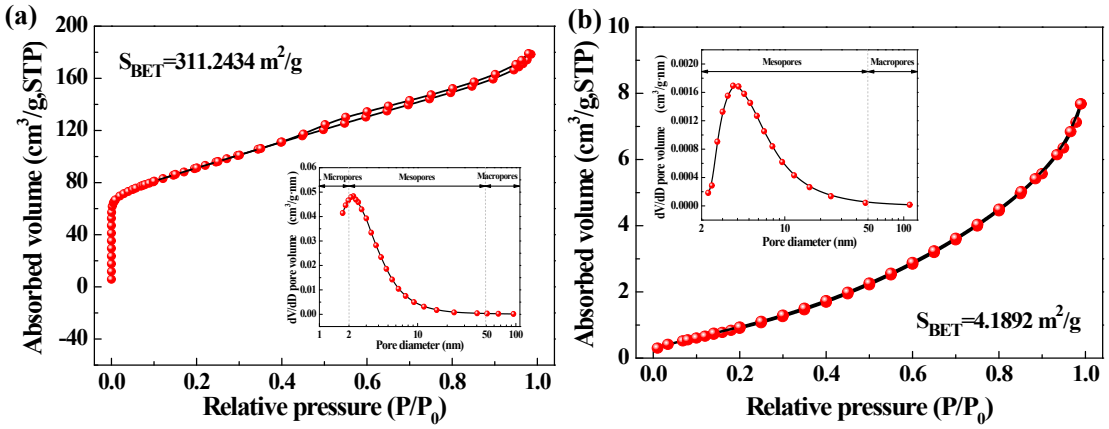

Fig. S5 N_2 adsorption-desorption isotherms and BJH pore-size distribution (from the adsorption branch of isotherms) of ZEO (a) and AZ (b).

As shown in Fig. S5, the isotherm of ZEO sample is identified as type IV, which is characteristic of mesoporous materials. The pore-size distribution obtained from the isotherm indicates a number of pores less than 10 nm in the ZEO sample. AZ sample with the feature of type II isotherm has only a negligible surface area of 4.1892 m^2 g^{-1}, which can be assigned to the physical adsorption on nonporous or macroporous materials. Most of the pores fall into the size range of 2 to 50 nm (mesopores region) in the AZ sample, which are mainly caused by the long and narrow gaps produced by the stacking of zirconia sheet layers.

3.2. Adsorption isotherms

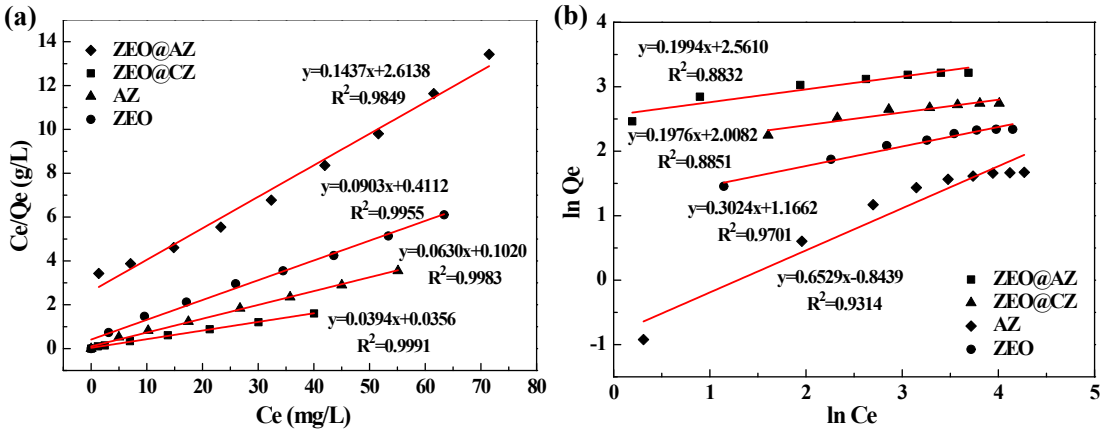

Fig. S6 Linearized Langmuir (a) and Freundlich (b) isotherm models for phosphates adsorption.

Fig. S6 illustrates the linearized Langmuir and Freundlich isotherm models for phosphates adsorption on various adsorbing materials, respectively. The slope and intercept of fitted equations are provided to calculate the relative parameters of the Langmuir and Freundlich adsorption isotherms. The correlation coefficients of fitted equations are used to measure the degree of linear dependence. By contrast, higher correlation coefficient (R^2>0.9849) indicates that Langmuir model is better fit the experimental data in this study.

3.3. Adsorption kinetics

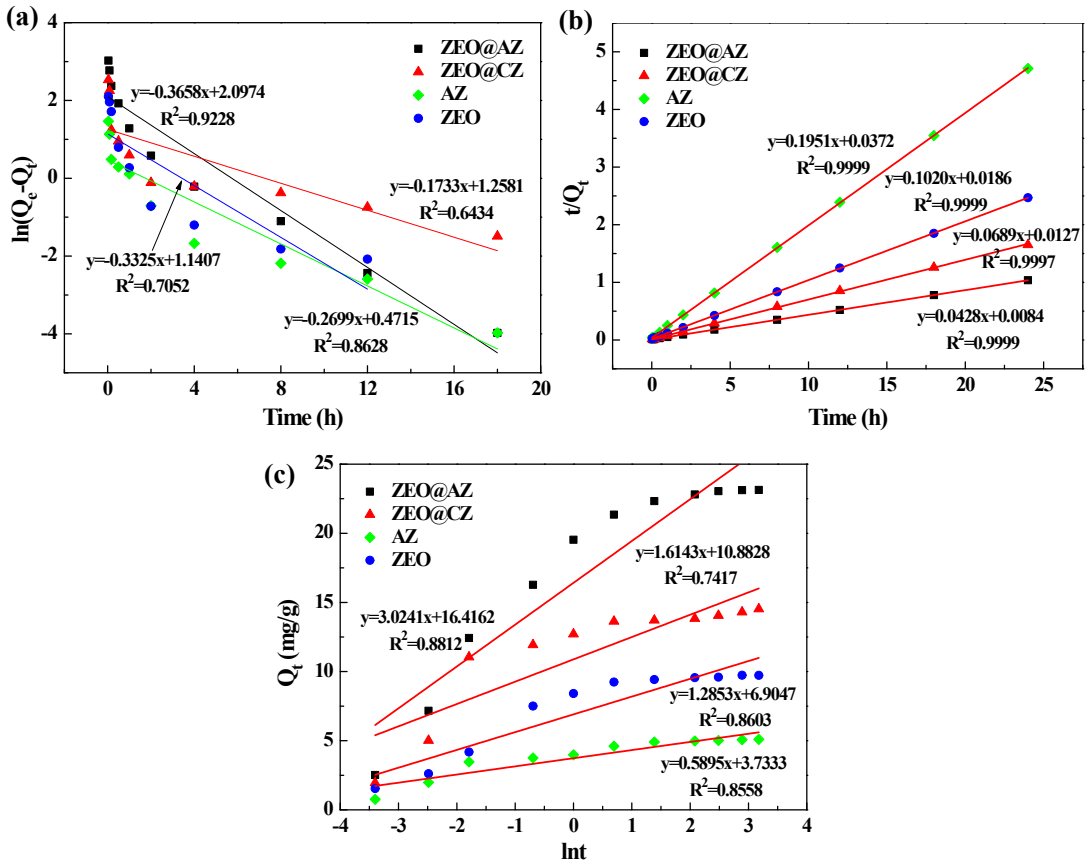

Fig. S7 Linearized kinetics models for phosphates sorption. Pseudo first-order model (a), pseudo second-order model (b) and Elovich model (c).

Fig. S7 shows the linearized pseudo first-order, pseudo second-order and Elovich models for phosphates adsorption on various adsorbing materials, respectively. The slope and intercept of fitted results are applied in calculating the relative parameters of kinetics models. The correlation coefficients of fitted curves are used to measure the degree of linear dependence. By contrast, higher correlation coefficient (R^2>0.9997) indicates that pseudo second-order model can better describe the phosphates adsorption on various adsorbents.

3.5. Effect of water quality on phosphates adsorption

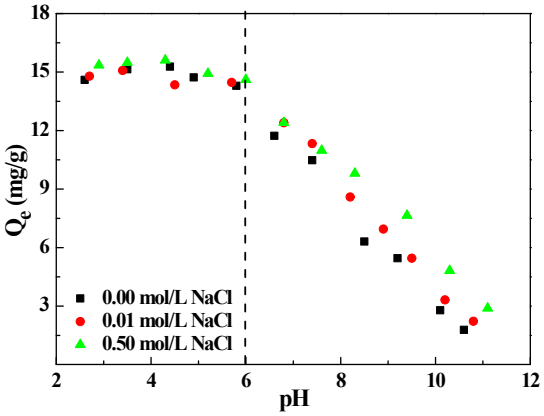

Fig. S8 Effect of solution pH and ionic strength on phosphates adsorption of ZEO@CZ.

As illustrated in Fig. S8, the ZEO@CZ also brings out the intense pH-dependency and ionic strength-dependency towards phosphates adsorption. In particular, the stable and efficient adsorption towards phosphates occur under acidic conditions with pH below 6, while the phosphates adsorption capacities significantly decrease with the increase in pH (>6), which is consistent with that of ZEO@AZ. Likewise, ionic strength also reveals the similar regularity with that of ZEO@AZ. Namely, the increase in ionic strength remarkably enhances the phosphates adsorption capacity of ZEO@CZ under neutral and alkaline solvent conditions, but has no obvious effect on that in acidic pH levels.

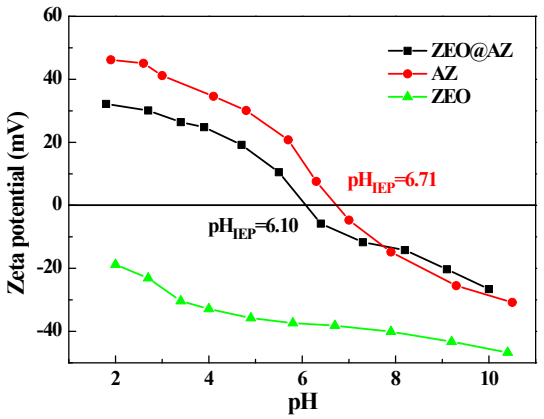

Fig. S9 Plots of Zeta potential of ZEO@AZ, AZ and ZEO samples with pH value.

As illustrated in Fig. S9, the Zeta potentials of ZEO@AZ, AZ and ZEO thoughout the pH ranges from 2 to 11 are -26.6~32.2 mV, -30.8~46.2 mV and -46.7~-18.8 mV, respectively. Specially, the isoelectric point (IEP) for ZEO@AZ and AZ are obtained at the pH of 6.10 and 6.71, whereas the ZEO exhibits the electronegativity throughout the pH range and has an insignificant impact on the IEP of ZEO@AZ. This result indicates that the amorphous ZrO_2 plays an important role in the surface electrical behavior of ZEO@AZ adsorbent compared with the negligible effect of zeolite.

3.7. Adsorption mechanism towards phosphates

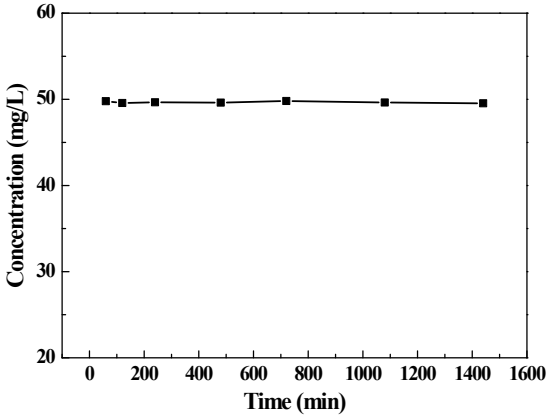

Fig. S10 Concentration change of phosphates solusion vs. time in the absence of sorbent.

Strictly speaking, phosphates are classified as being orthophosphates ($H_xPO_4^{(3-x)-}$), condensed phosphates (pyro-, meta- and other polyphosphates), and organic (or organically bound) phosphates [1]. They can occur in dissolved, particulate, and biological (within organisms) forms. In water quality analysis, however, phosphates are commonly referred to orthophosphates, whose concentration is mainly determined by Mo-Sb Anti-spectrophotometer method [2-4]. In order to evaluate the effect of possible polyphosphates on sorption mechanism, the control samples were used to conduct the adsorption experiment in the absence of sorbent for comparison. The details are as follows: 200 mL 50 mg L^{-1} KH_2PO_4 solution was put into a conical flask which was further placed in a thermostatic oscillator at 25 °C with the speed of 200 rpm for 24 h. At regular time intervals (60 min, 120 min, 240 min, 480 min, 720 min, 1080 min, 1440 min), the samples were taken out for phosphates concentrations analysis. The results showed that the phosphates concentration did not vary significantly in the absence of sorbent after the oscillation tests (Fig. S10), indicating that polyphosphates have a negligible impact on sorption process.

References

1. P. R. Rout, M. K. Shahid, R. R. Dash, P. Bhunia, D. Liu, S. Varjani, T. Zhang and R. Y. Surampalli, *J. Environ. Manag.*, 2021, **296**, 113246.
2. X. Zhu and J Ma, *Trends Anal. Chem.*, 2020, **127**, 115908.
3. E. A. Nagul, I. D. McKelvie, P. Worsfold and S. D. Kolev, *Anal. Chim. Acta*, 2015, **890**, 60-82.
4. H. Chen, L. Zhao, F. Yu and Q. Du, Analyst, 2019, **144(24)**, 7130-7148.